

Cite this: *Nanoscale*, 2023, **15**, 434

Reliability of printed stretchable electronics based on nano/micro materials for practical applications

Jian Lv, †^{a,b} Gurunathan Thangavel †^a and Pooi See Lee *^{a,b}

Recent decades have witnessed the booming development of stretchable electronics based on nano/micro composite inks. Printing is a scalable, low-cost, and high-efficiency fabrication tool to realize stretchable electronics through additive processes. However, compared with conventional flexible electronics, stretchable electronics need to experience more severe mechanical deformation which may cause destructive damage. Most of the reported works in this field mainly focus on how to achieve a high stretchability of nano/micro composite conductors or single working modules/devices, with limited attention given to the reliability for practical applications. In this minireview, we summarized the failure modes when printing stretchable electronics using nano/micro composite ink, including dysfunction of the stretchable interconnects, the stress-concentrated rigid–soft interfaces for hybrid electronics, the vulnerable vias upon stretching, thermal accumulation, and environmental instability of stretchable materials. Strategies for tackling these challenges to realize reliable performances are proposed and discussed. Our review provides an overview on the importance of reliable, printable, and stretchable electronics, which are the key enablers in propelling stretchable electronics from fancy demos to practical applications.

Received 15th August 2022,
Accepted 15th November 2022

DOI: 10.1039/d2nr04464a

rsc.li/nanoscale

1. Introduction

Stretchable electronics of a soft nature and with the capability to work under mechanical extension have been demonstrated for potential applications in wearable technologies,^{1,2} medical devices,³ soft robotics,^{4,5} and smart agriculture.^{6,7} Recent developments in soft sensors,^{8,9} soft energy devices,^{10,11} miniaturized IC chips,¹² and fabrication technology have enabled the promising possibilities of stretchable electronics which can deform along soft subjects.¹³ Among various fabrication techniques, the printing of stretchable electronics has been attracting considerable attention owing to its relatively low cost, scalable fabrication, lower material waste (additive manufacturing), and versatile material selection.^{12,14,15} The stretchability of printed electronics can be realized using intrinsically stretchable conductors or/and stretchable structures. Intrinsically stretchable materials utilize deformable/elastic materials or composites to endure the applied strain, while the structural designs, such as serpentine, kirigami structures, wrinkles, and arches, transfer the stretching strain to localized bending, buckling, or twisting.^{13,16} The inks formulated for

the printing of stretchable electronics can be stretchable conductive polymers,^{17,18} ionic gel/polymer,^{19,20} or composites with conductive fillers and elastomeric binders.²¹ Among these, inks comprising nano/micro conductive fillers and elastomeric binders are attracting considerable attention for the fabrication of stretchable electronics because of their high conductivity and stability, especially in metal-based inks.^{14,22–24} The translation to practical applications will hinge on the success in meeting the stability, durability, and reliability requirements for productization. In 2020, the market for stretchable electronics was about USD 16.5 million, and is expected to reach USD 2.6 billion in 2027.²⁵ To address potential market needs, the gap between lab prototype and product is still the biggest challenge that impedes the adoption of printed stretchable electronics.

Printed flexible electronics based on nano/micro composite inks are already mature technologies and have experienced a soaring gain in recent decades. The bending functionality has been addressed and does not cause severe damage to the thin-film electronics. The global market for flexible electronics in 2020 was USD 41.2 billion and is expected to increase to USD 74 billion in 2030.²⁶ When it comes to stretching deformation, the challenges are significantly elevated. There are already several reviews about the progress of printed stretchable electronics; they mainly focus on the realization of stretchability, including printed stretchable sensors,²⁷ energy devices,^{28,29} display^{30,31} and data transmission,³² and lack the overall evaluation of reliability from a system-level view. Even for the realization of

^aSchool of Materials Science and Engineering, Nanyang Technological University, 50 Nanyang Avenue, 639798, Singapore. E-mail: pslee@ntu.edu.sg

^bSingapore-HUJ Alliance for Research and Enterprise (SHARE), Smart Grippers for Soft Robotics (SGSR), Campus for Research Excellence and Technological Enterprise, Singapore 138602, Singapore

†These authors contributed equally to this work.

stretchability, these reviews mainly focus on the simple implementation of strain, and reliability aspects, such as the strain rate-dependent performance, are rarely discussed.^{22,33,34}

Considering the stretchability of entire systems and the impact of working environments, the challenges for producing reliable printed stretchable electronics become more complicated. Typically, stretchable devices are composed of stretchable sensors, displays, data transmitters and energy modules to realize sensing, visual showing, communication and power supply applications, respectively,³⁵ as shown in Fig. 1. The printable and stretchable nano/micro composite inks are core components to enable durability to deformation. Under stretching, the elastomeric binders bind the conductive fillers, while conductive fillers slide with each other but maintain the conductive networks. Current printed stretchable solid nano/micro composites still suffer from distinctive resistance increase upon stretching, especially for cycling and fast stretching, leading to the malfunction of entire circuits. As some components, such as data processors and standard resistors, are still in the rigid form, soft-rigid junctions are inevitable for hybrid stretchable electronics. The huge differences in Young's modulus cause the concentration of stress and lead to breaks in soft-rigid junctions. Like traditional rigid circuits, multilayer design can increase the areal density of components, which is valuable when the surface area of targeted subjects is limited. However, the filling materials in the vias that connect cross-layer circuits are subject to insufficient filling and component mismatch with the elastomeric substrate that significantly induces the resistance increase with

the implementation of strain. Beyond the challenges coming from stretching, damage can also be incurred from thermal accumulation and exposures in working environments. The thermal accumulation mainly results from the operation of the electronic components resulting in resistive heating, and is even more detrimental for printed stretchable electronics because elastomers that serve as the substrate and binder are poor thermal conductors, and some target applications involving living tissues are sensitive to high temperatures. The stability issue of the printed stretchable electronics not only involves the oxidation/corrosion of conductive fillers and the accelerated aging process of the elastomeric binders, but also concerns the stretchable encapsulation with an unfavorable transmittance for oxygen and water. The target to achieve reliable printed stretchable electronics requires mature practices and guidance for the stretchable system design and manufacturing.

In this review, we discuss the different failure modes of printed stretchable electronics, including the challenges in interconnects, soft-rigid connections, vias for multilayer electronics, heat dissipation, and stability of stretchable materials in the working environment, together with a summary of recent efforts and prospects on potential means to address these challenges to realizing reliable printed stretchable electronics. Stretching deformation causes severe disturbance to most electrically and thermally conductive matter. When integrating different components to form an electronic system, the interfaces and connectivity pose new challenges for maintaining integrity. Beyond the electromechanical challenges,

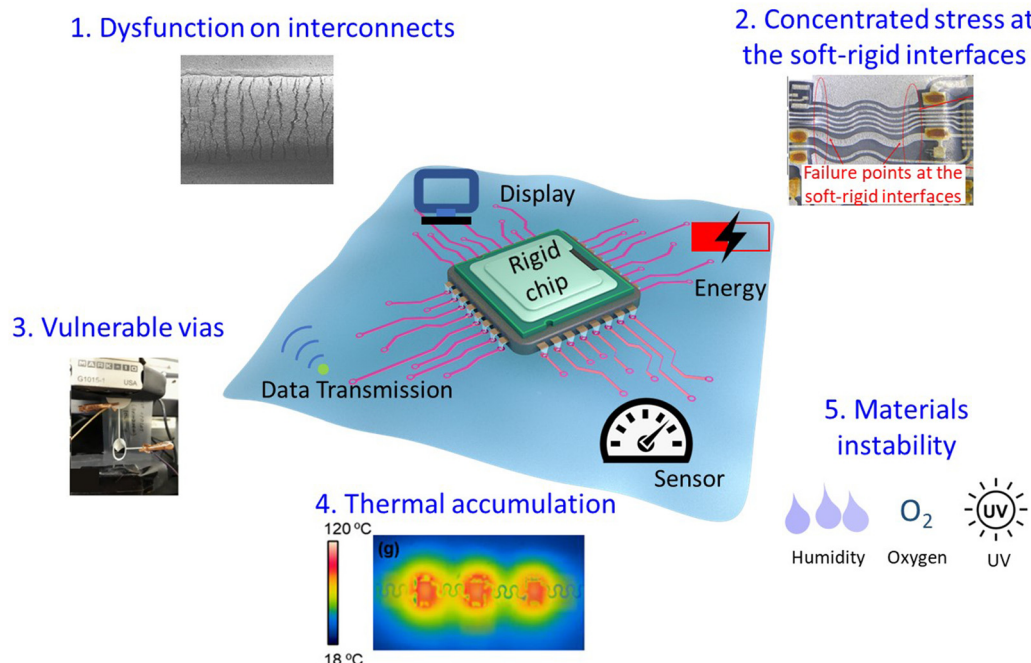


Fig. 1 The common failure modes, including dysfunction on interconnects, concentrated stress on the soft-rigid interfaces, vulnerable vias, thermal accumulation and instability of stretchable materials (reproduced with permission,⁹⁵ copyright 2021, IEEE; reproduced with permission,¹¹¹ copyright 2020, Springer; reproduced with permission,¹¹⁶ copyright 2021, Springer), and main components in printed stretchable electronics.



stretchable materials, including elastomeric binders and fillers, also face stability issues in working environments. Material optimization, structure design, and systematic considerations have been key factors in solving these problems in previous works and should be considered in future works. Lastly, our thoughts about the next steps for fostering the development of printed stretchable electronics will be presented.

2. Dysfunction of the stretchable interconnects

The inks formulated for the printing of stretchable electronics can be stretchable conductive polymers, ionic gel/polymer, or composites with conductive fillers and elastomeric binders.¹³ A comparison, including conductivity, stretchability and stability, among the three different conductors is shown in Table 1. The combination of polymer flexibility and metal conductivity enables conductive polymers with great promise in flexible electronics. The stretchability can also be endowed by involving additives, including plasticizers and polymers.¹⁷ The recent progress in stretchable conductive polymer has been reviewed in previous reviews.^{17,36} Similar to biosystems, the conductivity of stretchable ionic gels/polymers comes from the migration of the ions. As a result, ionic gels/polymers have shown great potential in bioelectronic and biomedical applications. Recent decades have witnessed the booming development of stretchable ionic gels/polymers in wearable and soft electronics.^{19,37,38} The inks composing the nano/micro conductive fillers and elastomeric binders deliver a higher conductivity and stability, and thus have been considered as the priority for the printing of stretchable circuits that meet the requirement for overall low resistance and a long operating life.^{21,22} Recently developed liquid metal nano/microparticles that can deform along the tensile strain direction have shown much less resistance increase upon stretching compared with the rigid nano/micro conductive fillers, attracting intensive efforts from researchers.^{39–42} However, the leakage issue and corrosive properties of liquid metal still affect its wide applications.

Here, we focus on the ink composed of solid nano/micro conductive fillers with elastomeric binders because of their ease of handling, high conductivity and stability, especially for metal-based inks. The conventional printed flexible conductors are accompanied by sintering treatment to reduce the elec-

tron transfer barrier, which is associated with partial/full removal of surfactant/binder and the connection of adjacent conductive fillers.^{53,54} However, printed stretchable conductors require a large proportion of elastomeric binder to resist cracking and hold the conductive fillers together when they slide with each other. This working mechanism determines that the conductivity of the printed stretchable conductor at a relaxed state is generally lower than that of conventional flexible conductors. Meanwhile, the resistance increment is often exceedingly high during stretching, as the overlapping and contact areas among conductive fillers are reduced when they are sliding along the stretching direction. The durability of cycling stretching is even more challenging; the viscoelastic property of elastomeric binder, the evolution of cracking, frictions among neighboring conductive fillers, and frictions between conductive fillers and binders make it hard to recover the conductive percolations and conductivity. The strain rate-dependent property of elastomeric binder makes the resistance increment sensitive to how fast the strain is implemented, which is unfavorable as the stretching speed is variable in practical applications.

Conductive nanomaterials, including metal nanoparticles,^{55–57} nanowires,^{58,59} carbon nanotubes (CNTs),^{60–62} graphene and nanocomposites/hybrids^{14,22} can be utilized to print stretchable interconnects; however, the cost of nanomaterials is still relatively high, and the process of formulation and printing of stretchable nano ink is often too complicated. Micro-sized materials are lower in cost and have good dispersion in various solvents, making them the right choice for scalable printed stretchable electronics.²¹ The mechanical property of the binders, the shape of the conductive fillers, and interactions between binders and conductive fillers determine the stretchability and electrical performance of the conductor. Micro-flakes, with their ease of forming conductive percolation, have been intensively applied for the formulation of printed stretchable ink.^{63,64} Some strategies to enhance the electrical and mechanical performance include the self-assembling of conductive materials on the surface to form a highly conductive surface and the incorporation of a highly stretchable polymer matrix underneath.^{50,65} However, the mobility of flakes is limited, and the capability to form conductive percolation is inferior compared with nanowires, which causes unsatisfactory stretchability. In this part, we mainly focus on using nanomaterials as additives to increase the performance of micro-sized materials for stretchable interconnects.

Table 1 The comparison among printed stretchable conductive polymeric, ionic gel/polymer, or nano/micro composite conductors

Stretchable conductor	Conductivity (S cm^{-1})	Stretchability (%)	Sheet resistance ($\Omega \square^{-1}$)	Stability	Printing	Ref.
Conductive polymers	0.1–4000	50–800	10–84	Sensitive to humidity, temperature	Inkjet, transfer, nozzle	17 and 43–46
Ionic gel/polymer	0.001	1000	100–1000	The ionic liquid easily leaks out	Inkjet, transfer	47 and 48
Nano/micro composite	100–10 000	100–1000	0.01–0.1	Stable	Screen, inkjet, nozzle	49–52



Nanoparticles can align and self-organize along the applied strain direction, thus can enhance the electron transfer pathways during stretching.⁶⁶ Directly adding the nanoparticles inside the ink composite has been proved to be an effective way to improve the conductivity at relaxed and stretched states, as the nanoparticles can bridge the adjunct Ag flakes at both states.⁶⁷ Further intense pulsed light (IPL) irradiation has been introduced to enhance the bonding among Ag nanoparticles and improve the conductivity in the relaxed state, but the R/R_0 during stretching was much higher, due to the partially weakened mobility of Ag nanoparticles caused by sintering. It is noteworthy that pure Ag micro flakes do not respond to IPL irradiation, as their surface energy is less than that of Ag nanoparticles and it is hard to realize the necking growth among Ag micro flakes. Matsuhisa *et al.* invented an easier way to incorporate Ag nanoparticles into the elastomer matrix through an *in situ* reaction among Ag flakes, fluorine surfactant, and fluorine rubber at a high temperature (120 °C), as shown in Fig. 2A.⁴⁹ The maximum initial conductivity and the conductivity at 400% stretching reached 6168 S cm⁻¹ and 935 S cm⁻¹ with a speed of 10% min⁻¹, respectively, demonstrating that the *in situ* formed Ag nanoparticles can significantly enhance both stretchability and conductivity. Guo *et al.* further expand this idea to remove dependence on the fluorine elastomer by pre-iodizing the surfactant on Ag flakes and subsequently exposing it to photoactivation after printing.⁶⁸ This method applies to various chemically and physically cross-

linked elastomers, broadening its application on different occasions. Recently, we utilized non-hazardous artificial real human sweat to *in situ* generate the Ag nanoparticles on the surface of the Ag flakes, as shown in Fig. 2B.⁶⁹ The coexistence of Cl⁻ and low pH works synergistically to partially remove the insulated surfactant and enhance the connection among exposed Ag flakes, thus significantly improving the conductivity of the printed Ag/hydrophilic poly(urethane-acrylate) (HPUA) electrode at both the relaxed and stretched states. The mild sweat solution enables *in situ* sintering on soft substrates, enriching the versatile methods of designing stretchable and wearable electronics.

Ag nanowires and carbon nanotubes are liable to form the network connecting the micro conductive fillers to improve the performance of printed stretchable conductors.^{70,71} For this method, it is preferred that the Ag nanowires/carbon nanotubes are randomly distributed and allow free movement during stretching, otherwise segregated bundles will appear and are liable to cause cracks. As shown in Fig. 2C, nonionic surfactant sorbitane monooleate (SPAN 80) was added to the matrix to reduce the bonding between the carbon nanotubes and Ag flakes.⁷¹ Recently, Ag nanoparticles, Ag nanowires, and Ag flakes were even combined in one stretchable conductor, as shown in Fig. 2D.⁵² With the surface modification by 1-decanethiol, three types of conductive fillers can readily rearrange the original percolations that can be maintained upon the strain. The conductivity is around 31 000 S cm⁻¹ with less than

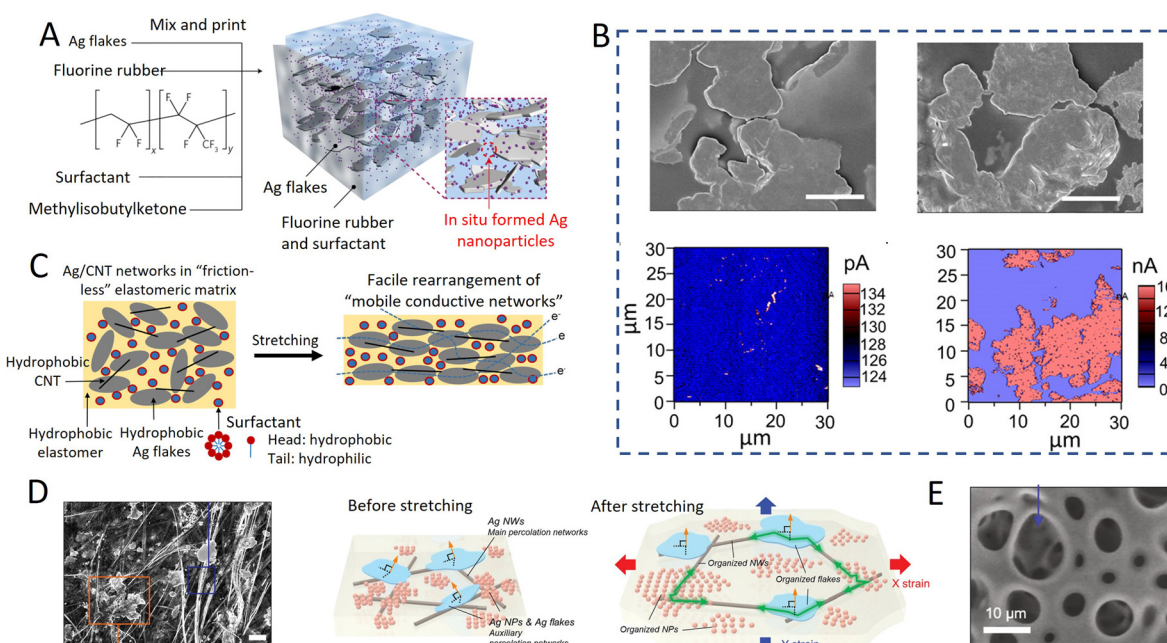


Fig. 2 The application of nanomaterials in enhancing the reliability of printed stretchable interconnects: (A) the *in situ* formation of Ag nanoparticle in the printed stretchable Ag flakes conductors, reproduced with permission,⁴⁹ copyright 2017, Springer Nature; (B) the sweat-induced sintering of printed stretchable Ag-HPUA conductor, reproduced with permission,⁶⁹ copyright 2021, American Association for the Advancement of Science; (C) the incorporation CNT to increase the stretchability of the Ag flakes conductors, reproduced with permission,⁷¹ copyright 2019, American Chemical Society; (D) the combination of Ag flakes, nanoparticles, and nanowires for the highly stretchable conductor, reproduced with permission,⁵² copyright 2022, Wiley-VCH; and (E) the porous PDMS elastomeric binder, reproduced with permission,⁷⁵ copyright 2021, Springer Nature.



1% change during the 50% uniaxial and biaxial stretching at a speed of 10 mm min^{-1} . This is the best performance so far for solid metal-based elastomeric conductors, but the printability of this method was not demonstrated and the loading of nano-materials is very high (90 wt%).

Most strategies for improving the performance rely on selecting or tuning the composition of the conductive fillers and modifying the interaction between conductive fillers and elastomeric binders. The maximum stretchability and conductivity are always the focus, but the cycling stretchability is unsatisfactory and the rate-dependent properties, which are also highly related to the hysteresis nature of elastomeric binders, are less studied. Even though chemically cross-linked elastomers, such as Eco-flex and polydimethylsiloxane (PDMS), have much smaller hysteresis loops than physically cross-linked elastomers, such as styrene-ethylene-butylene-styrene (SEBS) and thermoplastic polyurethane (TPU), they still suffer from poor performance during fast cycling stretching, especially with a high loading of conductive fillers.^{13,21,72-74} Most of the reported printed stretchable interconnects only delivered the stretching behavior at low strain rates, and the stretching rate-dependent property of printed nano/micro composite conductors has less been investigated. Elastomeric composite conductors still suffer from much more prominent resistance increases at a higher stretching speed, and this will affect the practical applications that undergo fast stretching speeds. These challenges may be solved by engineering elastomer binders with a porous structure,^{75,76} as shown in Fig. 2E. The porous binder can weaken the real strain by structural deformation along the stretching direction and weaken the propagation of cracks by blunting the tips of cracks.^{77,78}

3. Stress-concentrated rigid–soft interfaces

As rigid components, such as resistors and IC chips, are still unavoidable for typical device functions, the stress concentration in the junctions of soft and rigid components accounts for the major dysfunctions of the hybrid stretchable devices. Reliable conductive adhesive between the rigid components and stretchable interconnections is needed to guarantee effective electron transfer and strong bonding during the tensile load. Isotropic conductive adhesives (ICAs), instead of soldering, are the priority for connection because of the low-temperature process and environmental friendliness. Anisotropic conductive adhesives are required when the high-resolution circuit is designed.^{79,80} However, most of the present conductive adhesives face the challenge of having dual good bonding with both printed stretchable interconnects and rigid components. Fu *et al.* compared failure models of two types of ICAs during the rolling mechanical test in their work.⁸¹ The polyurethane-acrylic ICA has a strong bonding with the pins of the surface-mounted devices but delivered low adhesive force with printed Ag electrodes, whereas the polyurethane-based ICA showed the opposite behavior, making

them liable to fail along the ICA/stretchable Ag traces and ICA/rigid chips interface delamination, respectively. Traditional rigid ICAs based on epoxy and metal nano/microparticles have shown stable performance for rigid and printed flexible printed circuit boards (PCBs),^{82,83} but they have a huge mechanical property mismatch with the stretchable interconnects. Recent research about stretchable ICA is like that in printed stretchable interconnects; the conductivity and the stretchability are the main considerations.⁸⁴⁻⁸⁸ Adhesive inks composed of conductive fillers and elastomeric binders that are similar to that of printed stretchable interconnects would no doubt provide good adhesion with the printed stretchable interconnects as they share a similar composite and Young's modulus. However, the binding between rigid surface-mounted devices and stretchable ICAs has rarely been studied. The development of printed stretchable electronics needs a new conductive adhesive layer affording great bonding with both rigid parts and soft printed traces.

The conductive adhesive layer only can connect the rigid pins and printed stretchable interconnects. More steps are required to further stabilize the rigid parts on stretchable substrates. The strain localization method is commonly utilized by pre-stiffening the area and anchoring the rigid chips with a rigid supporting layer or rigid top encapsulation layer. Then the deformation upon stretching only happens on the printed stretchable interconnects. Yuan *et al.* utilized stiff PDMS with a high proportion of curing agent (16.7%) to encapsulate the rigid parts, and soft PDMS with a low loading of curing agent (6.3%) to protect printed stretchable interconnects, as shown in Fig. 3A.⁸⁹ The substrate, stiff encapsulation and soft encapsulation are the same type of polymer with Young's modulus variance, and thus enable great bonding between the different materials. The fabricated stretchable LED circuit containing a rigid resistor, a capacitor and a MCU chip can be stretched at 100%. This rigid island and soft bridge strategy was also applied in printing high-performance stretchable electrochemical devices, including biofuel cells and batteries.⁹⁰⁻⁹⁴

The concentrated stress and failures easily occur at the joint located between the rigid area and soft interconnects because of the huge mechanical mismatch. Behfar *et al.* printed a fully stretchable integrated ECG sensor for monitoring the body's physiological information, and used the stiff encapsulation on rigid components for achieving stable mounting.⁹⁵ Finite element modeling (FEM), which can predict the potential cracking points, is an effective tool in modeling the soft-rigid hybrid system with the presence of strain. As shown in Fig. 3B, the FEM result agrees well with experimental results; the crack density on the edges of the stiff encapsulant is much higher than that in printed stretchable interconnects. The cracking failures on the rigid–soft junctions made the wireless wearable ECG sensor lose function at 10% of tensile strain, though the printed interconnects can endure more stretching. This effect can be suppressed by widening the geometrical parameter of the printed stretchable interconnections at the soft-rigid transition area. Also, the shape optimization of rigid islands can change the distribution of



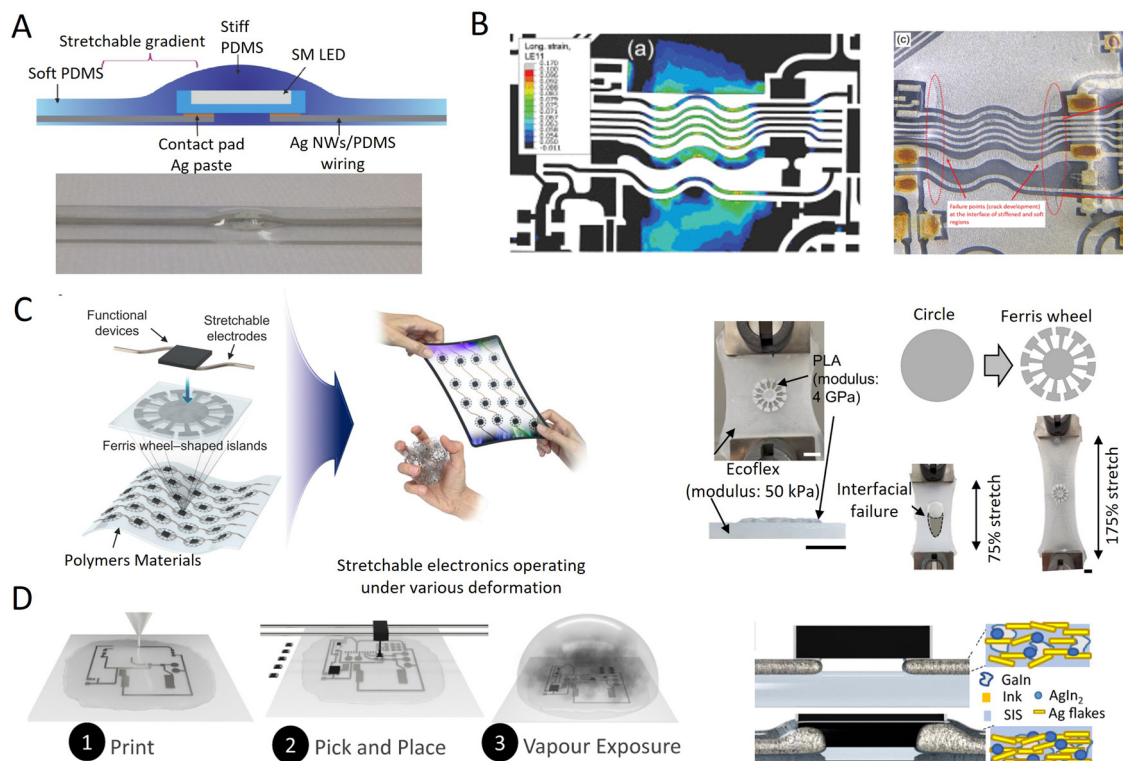


Fig. 3 Reliable rigid–soft junctions: (A) the utilization of rigid PDMS to stiffen the rigid LED chip in printed stretchable hybrid electronics, reproduced with permission,⁹⁹ copyright 2018, IOP science; (B) FEM simulation and real failures of printed stretchable hybrid electronics. Reproduced with permission,⁹⁵ copyright 2021, IEEE; (C) the complicated Ferris wheel-shaped rigid islands that can prevent the propagation of cracks at the rigid–soft interfaces. Reproduced with permission,⁹⁶ copyright 2022, American Association for the Advancement of Science; (D) the solvent vapor-induced soldering that connect the rigid chips and the soft interconnects for printed stretchable hybrid electronics, reproduced with permission,⁹⁷ copyright 2021, Springer Nature.

stress and improve the reliability of hybrid electronics. Yang *et al.* proposed one type of rigid island with a Ferris wheel shape which can significantly weaken the propagation of cracks at the rigid–soft junctions upon mechanical deformations,⁹⁶ as shown in Fig. 3C. The stretchability of the hybrid electronics was enhanced from 75% to 180% when the shape of the rigid bridge was changed from a circle to a Ferris wheel. The complex Ferris wheel changes the cracking path and improves the energy required for crack growth.

The property of the binder for printed stretchable electronics may offer a new method to connect the rigid parts and stretchable interconnects. Physically cross-linked elastomers are easily processed with the presence of dissolving solvents, which enables solvent-induced room-temperature soldering for printed stretchable hybrid electronics.⁹⁷ As shown in Fig. 3D, the entire circuit was put into the solvent vapor after printing the interconnects and mounting the rigid chip. Then the solvent vapor started to transfer the printed interconnects into a gel state, and rigid chips were surrounded by the gel interconnects. This method extended the maximum stretchability of printed hybrid stretchable electronics to >500%, which is more than enough for most application scenarios. However, solvent vapor-induced soldering is only applicable to physically cross-linked polymers, and the involvement of

liquid metal may erode the metal pins of rigid parts. EGaIn liquid metals have demonstrated great potential in realizing reliable soft–rigid connection upon stretching,^{98,99} but the encapsulation for preventing the oxidation of the liquid metal and inert interlayer for avoiding the corrosion on metal pins are required for long-time stability.^{100,101}

4. Vulnerable vias for multilayer electronics

Stretchable electronics with multi-layer configurations can realize the high-level integration of all components. This is valuable in applications with limited surface area for soft device mounting. For wearable epidermal sensing electronics, the multilayer design only requires contact between skin and sensing electrodes, and other components do not directly come into contact with the skin, increasing the safety of wearable electronics. However, the vias that realize the communications among different layers are vulnerable upon stretching due to component mismatch with the elastomeric substrate. Previous research on printed stretchable electronics has mainly focused on single-layer device fabrication, and the mature technologies for achieving reliable stretchable vias



await the right strategies. The process of forming the vias includes the generation of holes and the filling of the conductive materials. The hole size and shape significantly affect the reliability of the vias that electrically connect the circuits on the opposite sides of elastomeric substrates. The formation of the holes can be performed by either die cutting or laser ablation. Die cutting can only achieve cylindrical holes with a diameter of more than 100 μm . Conical via-holes, reproduced using laser-cutting, can keep the filling layer more reliably inside the via-holes rather than letting it flow through the hole, as compared with the punched or drilled cylindrical via-holes. Compared with die cutting, laser ablation has the advantage of achieving a high resolution. Meanwhile, laser ablation can be used to fabricate conical holes, making the filling ink stay inside the holes instead of flowing through.^{102–104} The ablation process relies on electron excitation in the substrate under laser irradiation to generate heat for the melt and evaporation of the polymer. In our previous work, the laser also could reduce graphene oxide and realize highly conductive and well-patterned electrodes for a stretchable supercapacitor.¹⁰⁵ Thorough information about polymer ablation can be found in an earlier review.¹⁰⁶ Here, we mainly focus on filling the conductive materials for highly conductive and reliable vias.

Rigid conductive materials have shown reliable performance to connect multilayer stretchable rigid metal intercon-

tions enabled by the serpentine structural design. High elastic modulus polymeric materials, such as epoxy and polyimide, were utilized to stiffen the area for vias to form a “rigid island” and avoid damage upon stretching. The island-bridge structure can redistribute strain on the interconnection area. Huang *et al.* developed a stable via through selective ablation on serpentine Cu foil-Ecoflex stretchable circuits and screen printing of $\text{Sn}_{42}\text{Bi}_{57.6}\text{Ag}_{0.4}$ solder paste, as shown in Fig. 4A. After printing, 150 °C heating was used to transfer the paste to rigid pillars and form good bonding with bottom Cu pads. The Cu pads were strengthened by the polyimide and thus the strain was mainly distributed elsewhere. By doing so, researchers realized strain-invariant vias cross-layers and highly stable 4-layer highly integrated and stretchable circuits that can perform multi-channel sensing and data transmission.¹⁰⁷ Another work utilized electrohydrodynamic (EHD) printing to pattern a low-melting-point alloy in an in-plane serpentine structure and vertical pillar as the stretchable interconnects and vias, respectively, as shown in Fig. 4B. The syringe was heated to 175 °C to enable the flowing of the alloy for printing. After printing, the molten alloy ink solidified on the substrate because the substrate temperature was lower than the melting point. This feature not only facilitated the printing of in-plane serpentine stretchable metal interconnects on soft PDMS, but also created the vertically printed alloy pillar for vias. A high-

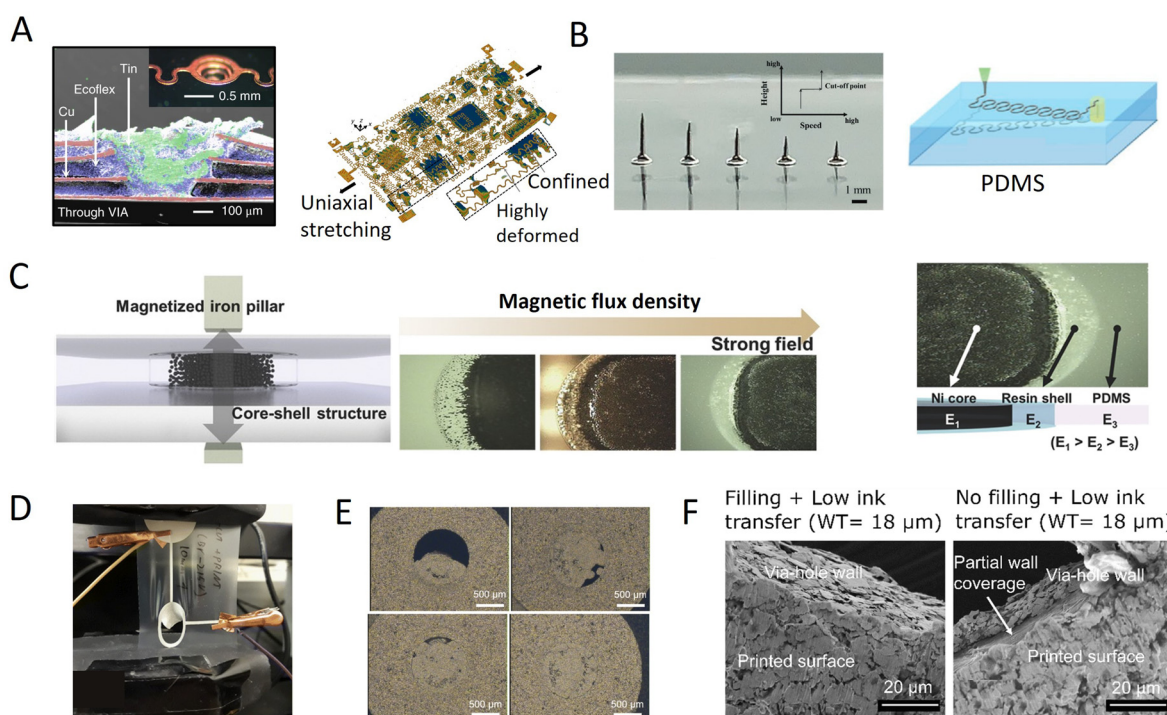


Fig. 4 Reliable vias for multilayer printed stretchable electronics: (A) the conventional solder paste as the via for connecting the multilayer stretchable Cu metallic electronics, reproduced with permission,¹⁰⁷ copyright 2018, Springer Nature; (B) electrohydrodynamic (EHD) printed low-melting-point alloy in in-plane serpentine structure and vertical pillar as the stretchable interconnects and vias, respectively, reproduced with permission,¹⁰⁸ copyright 2021, Wiley-VCH; (C) the magnetically aligned Ni particles–silicone composite as the vias for printed stretchable electronics, reproduced with permission,¹¹⁰ copyright 2017, Wiley-VCH; (D) the Ag stretchable inks as the via fabricated by printing and filling, reproduced with permission,¹¹¹ copyright 2020, Springer.



modulus epoxy was used to reduce the strain on the rigid metal via, increasing the tensile stretchability from 6% to 40%.¹⁰⁸

When the rigid composite was applied to function as the via, the resistance was much higher due to the coexistence of massive insulating polymer binder.^{109,110} Oh *et al.* formulated a nickel particle/rigid silicone ink in a weight ratio of 1:1 for connecting the electronic circuit on the opposite side of the PDMS substrate.¹¹⁰ The conductivity was around 3 S m^{-1} , which was much lower than the traditional metal vias. To reduce the resistance, magnetic alignment was applied to induce the concentrated nickel particle aggregation under the magnetic pillar, as shown in Fig. 4C. The vertical magnetic field realized a particle-rich area in the center and a polymer-rich area at the shell. Due to the compatible molecular structure of rigid silicone resin and PDMS, the bonding between rigid shell and substrate was robust. Not only was the resistance of vias significantly reduced, but the stretchability was also enhanced because the rigid polymer-rich shell could protect the particle-rich core free from mechanical deformation. Even with this design, the overall resistance of one via was still around 30Ω and awaits further reduction by a new design.

Compared with rigid conductive materials, deformable vias composed of conductive fillers and elastomeric binders offer better compatibility in Young's modulus with the stretchable substrate and printed soft conductors, and thus have greater potential in printed intrinsically stretchable electronics. However, the soft vias are more likely to fail upon stretching due to the presence of a high proportion of metal particles, as shown in Fig. 4D.¹¹¹ The formulation of some conductive ink/pastes involves solvent to tune the viscosity and flowability, which brings the challenge of achieving a high filling rate, as volume shrinkage is inevitable during the curing process. Thus, the filling process requires a higher volume of ink than that of the via holes. As shown in Fig. 4E, with the increased thickness of the screen for printing from $18 \mu\text{m}$ to $120 \mu\text{m}$, the filling effect was enhanced.¹¹¹ However, the increased thickness of the screen stencil reduces the resolution of the printing. Full coverage of the side wall instead of the whole area of a hole with conductive inks is enough to realize the cross-layer connection, as shown in Fig. 4F. This approach attains the substrate support for vias material and avoids the cracking associated with the larger area created by materials that fill the whole hole. However, the resistance of the via is still increased upon stretching, resulting from the basic electromechanical property of elastomer-conductive filler composite.

For future work, elastomeric binder without the solvent is preferable for filling the hole, as the volume will not shrink during the curing process. Silicone, including PDMS and Ecoflex, can be utilized to realize a high rate of filling. Meanwhile, a strategy is required to minimize the component mismatch between filling materials and substrates. The material property mismatch may induce the detachment of filling materials from the polymeric substrate upon stretching. It is noted that the experience in achieving the highly stretchable printed composite can be applied here to minimize the resistance increment when vias are stretched.

5. Thermal accumulation

Thermal management is one of the most critical issues for high-performance electronic devices. Researchers discovered that temperature is responsible for more than 55% of electrical component failures, with a $1 \text{ }^\circ\text{C}$ rise in temperature reducing dependability by 4% and a $10\text{--}20 \text{ }^\circ\text{C}$ increase doubling the failure rate.¹¹² As a result, electronic components needed an effective cooling system to maintain a safe working temperature.¹¹² Specifically, the thermal accumulation of stretchable electronics is even more detrimental, as most soft polymer substrates and targets for the application of stretchable electronics, such as the human body, are sensitive to high temperatures. Meanwhile, the thermal expansion of the elastomeric binder in printed composite conductors induces a significant resistance variance, which is called the temperature coefficient of resistance (TCR).¹¹³ The heat accumulations deteriorate the bonding between the soft and rigid parts, as escalated heat softens the elastomeric binders and thus weakens the adhesion and cohesion of the ICAs. As conductive vias often suffer from significant component mismatch with the elastomeric substrate, displacement between vias and substrates can result from the discrepancies in the thermal expansion coefficient upon accumulated heat. In addition, the oxidation of active conductive fillers can be accelerated by the increased temperature. Heat dissipation of printed stretchable electronics introduces significant difficulty in maintaining steady thermal conductivity under large deformation.¹¹⁴ Even though some stretchable electronics have utilized thermal management modules to dissipate the accumulation of heat and increase performance,^{115,116} high-performance printed stretchable electronics with superior heat management have not yet been revealed.

Achieving effective heat dissipation from a heat source requires a thermal interface material (TIM), which is a vital component in ensuring dependable and stable thermal dissipation from high-power devices.^{117\text{--}119} The primary objectives are to create TIM materials with a low temperature expansion coefficient (CTE), high thermal conductivity, lower dielectric constant, excellent electrical resistivity, ease of processing, and most critically high compatibility with printed stretchable electronic substrates. Ultimately, there is a trade-off between the high heat conductivity of a material and the soft dynamics that allow for its greater thermal coupling.¹²⁰ Typically, materials with strong bonds, such as ceramics and metal-bearing materials, have a high heat conductivity.¹²¹ Owing to their electrical insulation and durability, some ceramic materials with high thermal conductivity ($1\text{--}300 \text{ W m}^{-1} \text{ K}^{-1}$), such as silicon nitride (Si_3N_4), aluminum nitride (AlN), silicon carbide (SiC), and boron nitride (BN), have been widely investigated as fillers. Aluminum oxide (Al_2O_3 , $\sim 30 \text{ W m}^{-1} \text{ K}^{-1}$) is presently one of the most often utilized thermally conductive fillers due to its low cost and high electrical resistivity.¹²² Boron nitride is a kind of TIM filler that has been the subject of much research in recent years due to its high thermal conductivity ($100\text{--}600 \text{ W m}^{-1} \text{ K}^{-1}$) and dielectric properties.¹¹⁷ Metallic fillers with



greater thermal conductivity ($10\text{--}400\text{ W m}^{-1}\text{ K}^{-1}$) include aluminum (Al),¹²³ copper (Cu),¹²⁴ silver (Ag),¹²⁵ and nickel (Ni).¹²⁶ However, most filler materials are deemed unsuitable because their stiff structures may result in performance deterioration such as delamination, cracking, mechanical failure, and space formation.¹²⁷ Although adhesives and gels have strong mechanical responsiveness and have been used to repair poor interfaces and weak van der Waals bonding, they typically have limited heat conductivity.^{128\text{--}130}

In contrast, polymer-based TIMs are the most common choice because they can offer excellent interface contact and are soft and malleable enough to overcome several mechanical difficulties. The concept for the creation of soft elastomer-based heat transfer controls corrosion and fouling resistance. Commonly used polymer matrices include polyethylene,¹³¹ polyamide,¹³² polypropylene,¹³³ polyvinylchloride,¹³⁴ epoxy resins,¹³⁴ polycarbonate,¹³⁵ and silicone.¹³⁶ Among these materials, polyethylene (PE) nanofibers exhibited a thermal conductivity of $104\text{ W m}^{-1}\text{ K}^{-1}$, which is higher than the conductivities of approximately half of the metallic materials. It is anticipated that the nanoscale rearrangement of molecular chains by straining and flaws that diminish heat conductance may be minimized along the direction of stretching.¹³⁷ We previously investigated the influence of shear mixed EGaIn volume and anisotropy orientation. Thermal transport in microparticles with COOH-terminated polydimethylsiloxane (COOH-PDMS-COOH) composites was thoroughly investigated. It was observed that the composite's different anisotropy thermal transfer efficiency was created based on the stretching direction.¹³⁸ However, the fundamental problem in heat dissipation is that most soft polymeric matrix materials have inadequate natural thermal conductivity ($0.1\text{--}0.5\text{ W m}^{-1}\text{ K}^{-1}$).^{139\text{--}141}

To overcome this issue, composite materials packed with highly thermally conductive metallic or ceramic fillers have been constructed to suit the thermal conduction and dissipation requirements.^{142,143} The concern originates from the fact that the electrical properties of such nanocomposites are similar to filler qualities, but still, the production techniques and mechanical characteristics are closer to those of polymeric materials. It has been experimentally revealed that the effect of filler-polymer nanocomposite predominantly depends on various factors such as electrical conductivity, particle size and shape, volume fraction, and the spatial distribution of the metal particles.¹¹⁴ For example, recently Tan *et al.* reported the fabrication of a graphene nanoribbon (GNR) with boron nitride nanosheets (BNNSs)-containing TPU composites *via* a vacuum filtration deposition method.¹¹⁵ The resulting GNR/BNNS/TPU is a breathable, biocompatible strain sensor with exceptional temperature management capabilities. According to reports, the thermal conductivity of a sample comprising 35 wt% BNNSs and $50\text{ }\mu\text{g cm}^{-2}$ GNRs is $0.928\text{ W m}^{-1}\text{ K}^{-1}$, which is 2.42 times more than the heat conductivity of a sample containing 0 BNNSs and 50 g cm^{-2} GNRs ($0.383\text{ W m}^{-1}\text{ K}^{-1}$). Furthermore, they discovered a high interfacial heat conductance of $2.9\text{--}104\text{ W m}^{-1}\text{ K}^{-1}$ between both the

TPU-BNNS layer and air, demonstrating their device's outstanding thermal dissipation. The stretchable strain sensor showed long-term stability under 100% strain for more than 5000 cycles during the continuous straining cycles, which is critical for human-to-human skin attachment applications, making it a great choice for accurate human motion tracking (Fig. 5A). However, when it comes to the metal fillers, the higher loading amount of the metallic fillers in the polymeric matrix material is limited to some extent because of the simultaneously increased conductivity and stiffness of the composite.¹⁴⁴ Aside from all of these impressive qualities and prospective uses, intelligent printed electronics also present significant hurdles in how to increase the interface contact for phonon transfer at both the relaxed and stretched state.

The printed filler structure is extremely attractive for achieving high heat transfer performance in composite materials because it reduces the number of filler-polymer interfaces, preventing future polymer-filler heat transfer, and most importantly, energy is transmitted throughout filler skeletons.^{145,146} A complex network of filler skeletons offers adequate phonon transfer channels with plentiful interface points of contact, which might also efficiently play a vital role in improving the thermal conductance of polymeric composites.¹⁴⁷ These materials' attractiveness stems mostly from their large heat conductivities, significant specific surface regions, low weights, and outstanding overall capability.¹⁴⁸ In a study by Hu and coworkers,¹⁴⁹ an individual heat compliance textile based on thermal conductivity and highly aligned BN-PVA composite was manufactured through a minimal, quick, and expandable 3D printing method accompanied by a hot-drawing treatment, as shown in Fig. 5B. The heat transfer of the resulting BNNS/PVA fabric improved to $0.078\text{ W m}^{-1}\text{ K}^{-1}$, which is 2.2 and 1.6 times substantially larger than the heat transfer of cotton and PVA fabrics, respectively. The a-BN/PVA composite fabric's cooling impact is 55% more than that of commercial cotton fabric, indicating a superior thermal management application. The main benefit of this procedure is the material's stretchability and wearability. Meanwhile, these 3D-printed TIM can be stretchable without sacrificing the thermal conductivity by the structure design, such as a no-protruding kirigami structure, as shown in Fig. 5C.¹⁵⁰ The T-joint-cut kirigami made the non-extendable materials highly stretchable without detaching from the substrate.

In current stretchable electronics, thermally conductive elastomeric composites that combine outstanding stretchability with high thermal conductivity have long been sought.^{138,151} Similar to the stretchable electrically conductive composite, they suffer from insufficient initial low thermal conductivity and significant thermal resistance increase upon stretching (including the cycling stretching), due to the existence of massive elastomeric binders to maintain the stretchability and separation among fillers induced by mechanical deformation.¹¹⁴ Researchers can borrow the strategies of designing the printed stretchable conductors to enable both high stretchability and thermal conductivity, for example, the self-assembling of electrically/thermally conductive fillers and



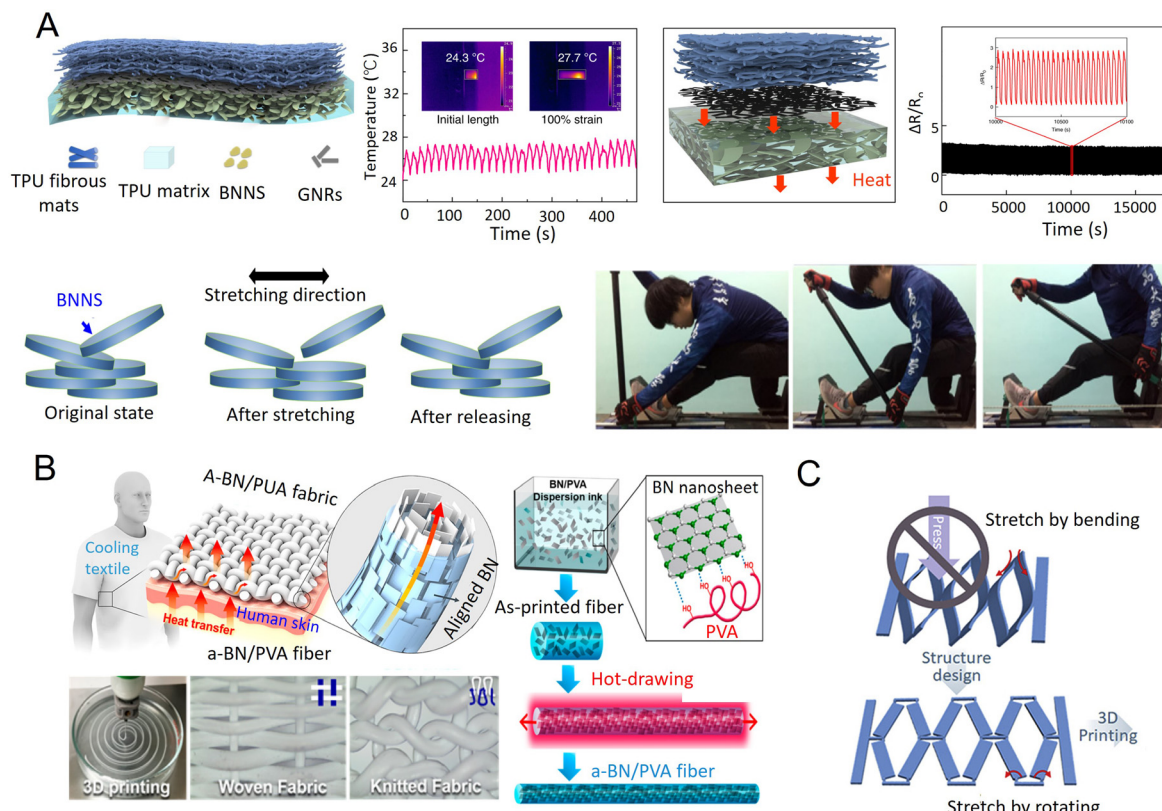


Fig. 5 TIM-based stretchable printable nanocomposite structures: (A) the stretchable sensor and the long-term cycling stability of the strain sensor under 100% strain for more than 5000 cycles, showing excellent stability and repeatability, reproduced with permission,¹¹⁵ copyright 2020, Springer Nature; (B) the fabrication process of a-BN/PVA composite fiber and optical images of the different fabric structures, reproduced with permission,¹⁴⁹ copyright 2017, American Chemical Society; (C) the T-joint-cut kirigami structure with non-protruding stretchability, reproduced with permission,¹⁵⁰ copyright 2020, Elsevier.

surface functionalization of the fillers. Beyond considering the thermal conductivity and stretchability, the effect of the thermally conductive layer on the performance of whole devices should also be studied. The involvement of the thermal conductive fillers increases the elastic modulus of elastomers and thus may sacrifice the softness of the whole stretchable device. When applying electrically conductive particles as thermally conductive fillers, the amount of fillers should be well controlled to avoid the short circuit in insulating layers.

6. Instability of stretchable materials

Compared with conventional printed flexible conductors, the printed intrinsically stretchable conductor involves different materials, which may introduce new challenges in realizing similar stability. The challenge escalates when some stretchable electronic devices are applied in the biomedical area and directly in contact with biofluids. Biofluids are composed of water, ions, oxygen, biomolecules, and tissues, and thus cause threats to the stability of the printed stretchable electronics that contain moisture-sensitive materials, such as metal conductive fillers. If the metal conductive fillers are eroded by bio-

fluids then some released metal ions, for example Ag^+ , could induce toxicity in the bio tissues. Elastomers are necessary for binding the conductive particles during stretching, and thus the stability of the elastomeric polymer should raise concerns. Elastomeric polymers are sensitive to heat, limiting their application in situations with a high surrounding temperature. Some of them, such as TPU and block copolymer elastomers, even suffer from the aging process in an environment with the presence of UV light, oxygen, and moisture.^{152,153} Meanwhile, most elastomers are permeable to moisture and oxygen, causing damage to the inner, easily oxidized, metal fillers.^{154,155} Even though most works have demonstrated the utilization of elastomers to encapsulate the printed stretchable circuit, long-term resilience to the working environment has not been demonstrated. Efforts to enhance the stability of the elastomeric binder have attracted much less attention from researchers. Surface modification, doping with inorganic particles, and molecular chain grafting are strategies that may significantly increase the stability of elastomeric binders.

Conductive materials, such as room-temperature EGaIn liquid metal, have been investigated for the delivery of stable electromechanical properties. Liquid metal is in the liquid form, but with metal conductivity, making it superior in the



printing of stretchable conductors. Printed liquid metal-based traces have been applied in ultra-stretchable conductors,^{156,157} vias,^{98,158} and anisotropic conductive adhesives with minimal resistance variation upon mechanical stretching.⁷⁹ However, liquid metal is sensitive to oxidation, destructive to IC chip metal pins and liable to leak.⁴⁰ Special measures should be taken to solve the challenge of liquid metals-based printed conductors. Inert carbon materials, including carbon nanotubes and graphene, have served as the interlayer to prevent the penetration of liquid metal into other metals.^{100,101} The success of liquid metal will change the way stretchable electronics are manufactured. When considering biomedical applications, conductive materials need a much higher resilience to oxidation and corrosion. Gold and carbon nano/micro materials are considered ideal chemically inert conductive fillers in biofluids and electrochemical reaction systems. However, gold-based nano/micro materials suffer from high costs, while carbon materials deliver insufficient conductivity for devices requiring a low overall circuit resistance. The coating of inert materials on the surface of Ag nano/micro-particles is still considered a potential method to realize both high conductivity and long-term stability in biofluids or electrochemical reactions. After electro-plating with Au, Ag flakes-based printed stretchable electrodes have demonstrated applications in sensing epicardial ECG⁷⁵ and electroretinogram signals from human eyes.¹⁵⁹ Au-coated Ag nanowires conductors also have shown good biocompatibility with a conductivity of $41\ 850\ S\ cm^{-1}$.¹⁶⁰ For electrochemical applications, Ag nanowires have been coated with Pt, Au, Pd, Fe, Ni, and PEDOT:PSS to realize stretchable sensing,¹⁶¹ energy storage^{162,163} electro-chemiluminescence¹⁶⁴ and electrochromic smart windows.^{165–167}

Elastomers, as binders for printed stretchable electronics, inevitably suffer from significant mechanical performance changes, and some even form color change, with continuous exposure to surrounding environments. Research in elastomers has intensively studied weathering tests (humidity, temperature, UV, ions) for various commonly used elastomers,

including TPU,^{168–171} silicone rubbers,^{172–174} and block copolymers.^{175,176} However, weathering tests for printed stretchable composite conductors have rarely been reported. The incorporation of conductive nano/microparticles may increase the durability of elastomers to aging. For example, carbon black and nanotubes can serve as a photostabilizer to interact with irradiation-generated free radicals, filter and disperse UV energy,^{153,177} thus enhancing the resistance to UV irradiation. Weathering tests of printed stretchable electronics that well consider the working environment are urgently needed.

Stretchable encapsulation is required for printed stretchable electronics to prevent the short-circuit, oxidation and leaking of metal ions. The commonly utilized elastomeric binders face challenges in serving as hermetic seals, though most of the reported works have applied them as encapsulations.¹⁷⁸ An ideal encapsulation can simultaneously maintain stretchability and protect the inner materials from the attack of ions and oxygen, thus enabling the wide selection of stretchable conductive materials in harsh working environments, for example, human biofluids. Unfortunately, the stretchability and permeability of small molecules are highly linked. Elastomers contain cross-linked or entangled 3D chain networks, and each chain continuously experiences thermal motion, and thus small molecules such as water and oxygen can easily diffuse through them. The permeability to oxygen and water of different materials can be found in Fig. 6. Inorganics, metals, graphene, and plastics have better resistance to oxygen and water transfer. Le Floch *et al.* laminated a layer of stretchable SiO_2 enabled buckling structure on the surface of PDMS film to decrease the transmissibility of water and air.¹⁷⁹ Yin *et al.* deposited Au on elastomeric SEBS film to prevent the leaching of the water from electrolyte, thus elongating the life of their printed stretchable AgO-Zn batteries.¹⁸⁰ Among elastomers, butyl rubbers show the best performance in resisting the transfer of oxygen and water, because the thermal motion of the network chains was impeded by methyl groups.¹⁸¹ As a result, less free space is available for small

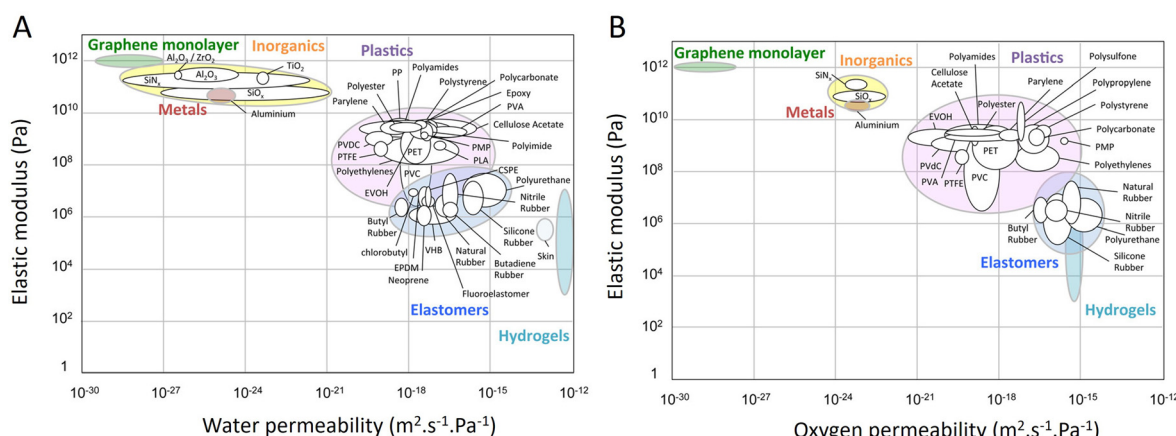


Fig. 6 The water and oxygen permeability of different materials.¹⁷⁹ Copyright 2018, American Chemical Society.



Table 2 The types of failures, causes, overcoming strategies and future trends of printed stretchable electronics

Type of failures	Causes	Overcoming strategies	Future trend
Dysfunction on interconnects	Conductive network change and viscoelasticity of elastomers	Conductive additives and fillers/elastomer interaction	Less strain rate-dependent and highly durable in cycling stretching
Concentrated stress at the soft-rigid interfaces	Steep jump of Young's modulus	Stretchable conductive adhesives and geometric design	Robust bonding with both rigid and soft components
Vulnerable vias	Low filling efficiency and material mismatch	Rigid via, component gradient and side wall coating	Solvent-free and soft filling and sealable fabrication
Thermal accumulation	Running of electronic circuit	Thermal dissipation substrate	Soft and highly conductive thermal interface materials
Materials instability	Active fillers; aging and high oxygen/water transmittance of elastomers	The surface modification, doping, and chain grafting	Incorporating printability to present strategies

molecules to transfer through the film. Butyl rubbers have been applied to protect stretchable organic electronic materials,^{182,183} triboelectric nanogenerators,¹⁸⁴ alternating current electroluminescence devices¹⁸⁵ and iongels.¹⁸⁶ However, few of the aforementioned strategies have been applied to printed stretchable electronics. Researchers in printed stretchable electronics need to pay more attention to the stability issue of their materials' selection, including conductive fillers, elastomeric binders and stretchable encapsulation based on the specific application scenarios of their soft devices.

7. Conclusion and perspective

Compared with printed flexible electronics, printed stretchable electronics are still in the infant stage of readiness for commercialization. The physical softness and capability of working under mechanical deformation make this technology a promising platform for solving the challenges in curved-surface and soft subjects. Apart from the stretchability of materials, systematic materials' properties consideration is required to realize stable performance in practical applications. Thus, the combination of new mechanisms, materials, and structure design is inevitable in increasing the reliability of the stretchable system under deformation. In this review, we have summarized the common failure modes in printed stretchable electronics and discussed the strategies for addressing these challenges. Future research should pay more attention to all factors that affect the reliability of the whole system upon stretching.

Stretchability is an attractive property for biomedical devices, soft robotics, smart agriculture, and human-machine interfaces. However, the stretching causes a huge challenge to the whole system of the electronics, including dysfunction of the conductors, separation of the rigid and soft parts, unstable communication among layers and thermal accumulation. These failures are even aggravated with fast-cycling stretching because the elastomers involved in the fabrication of printed stretchable electronics deliver a viscoelastic behavior, significantly affecting the restoration of the conductive networks after stretching. In addition to these physical dysfunctions, the selection of the material that enables the stretchability and

their application environments also cause concerns for their long-term stability. Some conductive fillers deliver attractive electromechanical properties, but their stability is still unsatisfactory, especially in the presence of biofluids. Elastomeric binders enable the elongation of printed electronics, but their durability to aging still cannot be ignored. Meanwhile, the stretchable encapsulations that require both stretchability and a low transmissivity to oxygen and water still lack systematic study. The types of failures, causes, the overcoming strategies and future trends are summarized in Table 2.

Beyond the points we have discussed, more breakthroughs are required for the right solutions, including international standards to evaluate the reliability of printed stretchable electronics. Even though research into stretchable electronics is flourishing around the world, the ways of evaluating performance has varied with different papers. It is a challenge to produce a fair and standard comparison among different research works. Meanwhile, the IC chips for the present stretchable electronics are still based on the conventional printed circuit boards which have a narrow tolerance for resistance variance. The IPC-9701 defined the failure of conductors as the reading of resistance change of more than 20% for more than 6 times,¹⁸⁷ which means most present printed stretchable conductors cannot meet this criterion. Thus it is highly desirable that IC chips or circuit designs that can work under a high resistance change to have a good match with the printed stretchable conductors. We believe that the success of printed stretchable electronics is revolutionary and will give us a new capability to sense, engage and connect with the world that we have not experienced before.

Conflicts of interest

The authors declare no conflict of interest.

Acknowledgements

This work is supported by the National Research Foundation, Prime Minister's Office, Singapore under its Campus of Research Excellence and Technological Enterprise (CREATE) program, Smart Grippers for Smart Robotics (SGSR).



References

1 K. K. Kim, Y. Suh and S. H. Ko, *Adv. Intell. Syst.*, 2021, **3**, 2000157.

2 J. Lv, C. Kong, C. Yang, L. Yin, I. Jeerapan, F. Pu, X. Zhang, S. Yang and Z. Yang, *Beilstein J. Nanotechnol.*, 2019, **10**, 475–480.

3 Y. J. Hong, H. Jeong, K. W. Cho, N. Lu and D.-H. Kim, *Adv. Funct. Mater.*, 2019, **29**, 1808247.

4 N. Lu and D.-H. Kim, *Soft Robot.*, 2014, **1**, 53–62.

5 J. Wang, D. Gao and P. S. Lee, *Adv. Mater.*, 2021, **33**, 2003088.

6 Y. Zhao, S. Gao, J. Zhu, J. Li, H. Xu, K. Xu, H. Cheng and X. Huang, *ACS Omega*, 2019, **4**, 9522–9530.

7 H. Yin, Y. Cao, B. Marelli, X. Zeng, A. J. Mason and C. Cao, *Adv. Mater.*, 2021, **33**, 2007764.

8 D. Gao, K. Parida and P. S. Lee, *Adv. Funct. Mater.*, 2020, **30**, 1907184.

9 J. Wang, M.-F. Lin, S. Park and P. S. Lee, *Mater. Today*, 2018, **21**, 508–526.

10 X. Gong, Q. Yang, C. Zhi and P. S. Lee, *Adv. Energy Mater.*, 2021, **11**, 2003308.

11 J. Lv, J. Chen and P. S. Lee, *SusMat*, 2021, **1**, 285–302.

12 J. Shalf, *Philos. Trans. R. Soc., A*, 2020, **378**, 20190061.

13 D. C. Kim, H. J. Shim, W. Lee, J. H. Koo and D.-H. Kim, *Adv. Mater.*, 2020, **32**, 1902743.

14 N. Zavanelli and W.-H. Yeo, *ACS Omega*, 2021, **6**, 9344–9351.

15 Z. Cui, *Sci. China: Technol. Sci.*, 2019, **62**, 224–232.

16 L. Yin, J. Lv and J. Wang, *Adv. Mater. Technol.*, 2020, **5**, 2000694.

17 L. V. Kayser and D. J. Lipomi, *Adv. Mater.*, 2019, **31**, 1806133.

18 M. Criado-Gonzalez, A. Dominguez-Alfaro, N. Lopez-Larrea, N. Alegret and D. Mecerreyres, *ACS Appl. Polym. Mater.*, 2021, **3**, 2865–2883.

19 H.-R. Lee, C.-C. Kim and J.-Y. Sun, *Adv. Mater.*, 2018, **30**, 1704403.

20 S. Park, K. Parida and P. S. Lee, *Adv. Energy Mater.*, 2017, **7**, 1701369.

21 N. Matsuhsisa, X. Chen, Z. Bao and T. Someya, *Chem. Soc. Rev.*, 2019, **48**, 2946–2966.

22 Q. Huang and Y. Zhu, *Adv. Mater. Technol.*, 2019, **4**, 1800546.

23 S. Choi, S. I. Han, D. Kim, T. Hyeon and D.-H. Kim, *Chem. Soc. Rev.*, 2019, **48**, 1566–1595.

24 G. Yun, S.-Y. Tang, H. Lu, S. Zhang, M. D. Dickey and W. Li, *Small Sci.*, 2021, **1**, 2000080.

25 R. and M. Ltd, Stretchable Electronics - Global Market Trajectory & Analytics, <https://www.researchandmarkets.com/reports/4845901/stretchable-electronics-global-market>, (accessed July 23, 2022).

26 R. Das, and X. He, *Flexible, Printed and Organic Electronics 2020–2030: Forecasts, Technologies, Markets*, 2019.

27 K. Senthil Kumar, P.-Y. Chen and H. Ren, *Research*, 2019, **2019**, 1–32.

28 X. Zhou and P. S. Lee, *EcoMat*, 2021, **3**, e12098.

29 S. Zhang, Y. Liu, J. Hao, G. G. Wallace, S. Beirne and J. Chen, *Adv. Funct. Mater.*, 2022, **32**, 2103092.

30 J. H. Koo, D. C. Kim, H. J. Shim, T.-H. Kim and D.-H. Kim, *Adv. Funct. Mater.*, 2018, **28**, 1801834.

31 J. Wang and P. S. Lee, *Nanophotonics*, 2017, **6**, 435–451.

32 S. G. Kirtania, A. W. Elger, M. R. Hasan, A. Wisniewska, K. Sekhar, T. Karacolak and P. K. Sekhar, *Micromachines*, 2020, **11**, 847.

33 D. F. Fernandes, C. Majidi and M. Tavakoli, *J. Mater. Chem. C*, 2019, **7**, 14035–14068.

34 W. Wu, *Sci. Technol. Adv. Mater.*, 2019, **20**, 187–224.

35 L. Yin, M. Cao, K. N. Kim, M. Lin, J.-M. Moon, J. R. Sempionatto, J. Yu, R. Liu, C. Wicker, A. Trifonov, F. Zhang, H. Hu, J. R. Moreto, J. Go, S. Xu and J. Wang, *Nat. Electron.*, 2022, 1–12.

36 B. C. K. Tee and J. Ouyang, *Adv. Mater.*, 2018, **30**, 1802560.

37 W. Niu and X. Liu, *Macromol. Rapid Commun.*, 2022, **43**, 2200512.

38 D. Gao, J. Lv and P. S. Lee, *Adv. Mater.*, 2022, **34**, 2105020.

39 M. Park, J. Park and U. Jeong, *Nano Today*, 2014, **9**, 244–260.

40 M. D. Dickey, *Adv. Mater.*, 2017, **29**, 1606425.

41 S. Chen, H.-Z. Wang, R.-Q. Zhao, W. Rao and J. Liu, *Matter*, 2020, **2**, 1446–1480.

42 C. Majidi, K. Alizadeh, Y. Ohm, A. Silva and M. Tavakoli, *Flexible Printed Electron.*, 2022, **7**, 013002.

43 Y. Wang, C. Zhu, R. Pfattner, H. Yan, L. Jin, S. Chen, F. Molina-Lopez, F. Lissel, J. Liu, N. I. Rabiah, Z. Chen, J. W. Chung, C. Linder, M. F. Toney, B. Murmann and Z. Bao, *Sci. Adv.*, 2017, **3**, e1602076.

44 Y. Yang, G. Zhao, X. Cheng, H. Deng and Q. Fu, *ACS Appl. Mater. Interfaces*, 2021, **13**, 14599–14611.

45 L.-W. Lo, J. Zhao, H. Wan, Y. Wang, S. Chakrabartty and C. Wang, *ACS Appl. Mater. Interfaces*, 2021, **13**, 21693–21702.

46 P. Tan, H. Wang, F. Xiao, X. Lu, W. Shang, X. Deng, H. Song, Z. Xu, J. Cao, T. Gan, B. Wang and X. Zhou, *Nat. Commun.*, 2022, **13**, 358.

47 S. Li, Y. Li, Y. Wang, H. Pan and J. Sun, *CCS Chem.*, 2021, **4**, 3170–3180.

48 D. Gao, J. Wang, K. Ai, J. Xiong, S. Li and P. S. Lee, *Adv. Intell. Syst.*, 2020, **2**, 2000088.

49 N. Matsuhsisa, D. Inoue, P. Zalar, H. Jin, Y. Matsuba, A. Itoh, T. Yokota, D. Hashizume and T. Someya, *Nat. Mater.*, 2017, **16**, 834–840.

50 N. Matsuhsisa, M. Kaltenbrunner, T. Yokota, H. Jinno, K. Kuribara, T. Sekitani and T. Someya, *Nat. Commun.*, 2015, **6**, 7461.

51 T. Wang, Q. Liu, H. Liu, B. Xu and H. Xu, *Adv. Mater.*, 2022, **34**, 2202418.

52 D. Jung, C. Lim, C. Park, Y. Kim, M. Kim, S. Lee, H. Lee, J. H. Kim, T. Hyeon and D.-H. Kim, *Adv. Mater.*, 2022, **34**, 2200980.

53 A. Kamyshny and S. Magdassi, *Chem. Soc. Rev.*, 2019, **48**, 1712–1740.



54 A. Kamyshny and S. Magdassi, *Small*, 2014, **10**, 3515–3535.

55 M. Tavakoli, M. H. Malakooti, H. Paisana, Y. Ohm, D. Green Marques, P. Alhais Lopes, A. P. Piedade, A. T. de Almeida and C. Majidi, *Adv. Mater.*, 2018, **30**, 1801852.

56 A. Shankar, E. Salcedo, A. Berndt, D. Choi and J. E. Ryu, *Adv. Compos. Hybrid Mater.*, 2018, **1**, 193–198.

57 S. Zhao, J. Li, D. Cao, Y. Gao, W. Huang, G. Zhang, R. Sun and C.-P. Wong, *J. Mater. Chem. C*, 2016, **4**, 6666–6674.

58 J. Xiong, S. Li, Y. Ye, J. Wang, K. Qian, P. Cui, D. Gao, M.-F. Lin, T. Chen and P. S. Lee, *Adv. Mater.*, 2018, **30**, 1802803.

59 J. Liang, K. Tong and Q. Pei, *Adv. Mater.*, 2016, **28**, 5986–5996.

60 J. Lv, I. Jeerapan, F. Tehrani, L. Yin, C. A. Silva-Lopez, J.-H. Jang, D. Joshua, R. Shah, Y. Liang, L. Xie, F. Soto, C. Chen, E. Karshalev, C. Kong, Z. Yang and J. Wang, *Energy Environ. Sci.*, 2018, **11**, 3431–3442.

61 I. Jeerapan, J. R. Sempionatto, A. Pavinatto, J.-M. You and J. Wang, *J. Mater. Chem. A*, 2016, **4**, 18342–18353.

62 A. J. Bandodkar, I. Jeerapan, J.-M. You, R. Nuñez-Flores and J. Wang, *Nano Lett.*, 2016, **16**, 721–727.

63 O.-H. Huttunen, T. Happonen, J. Hiitola-Keinänen, P. Korhonen, J. Ollila and J. Hiltunen, *Ind. Eng. Chem. Res.*, 2019, **58**, 19909–19916.

64 J. Suikkola, T. Björninen, M. Mosallaei, T. Kankkunen, P. Iso-Ketola, L. Ukkonen, J. Vanhala and M. Mäntysalo, *Sci. Rep.*, 2016, **6**, 25784.

65 T. Wang, Q. Liu, H. Liu, B. Xu and H. Xu, *Adv. Mater.*, 2022, **34**, 2202418.

66 Y. Kim, J. Zhu, B. Yeom, M. Di Prima, X. Su, J.-G. Kim, S. J. Yoo, C. Uher and N. A. Kotov, *Nature*, 2013, **500**, 59–63.

67 I. Kim, K. Woo, Z. Zhong, P. Ko, Y. Jang, M. Jung, J. Jo, S. Kwon, S.-H. Lee, S. Lee, H. Youn and J. Moon, *Nanoscale*, 2018, **10**, 7890–7897.

68 W. Guo, P. Zheng, X. Huang, H. Zhuo, Y. Wu, Z. Yin, Z. Li and H. Wu, *ACS Appl. Mater. Interfaces*, 2019, **11**, 8567–8575.

69 J. Lv, G. Thangavel, Y. Li, J. Xiong, D. Gao, J. Ciou, M. W. M. Tan, I. Aziz, S. Chen, J. Chen, X. Zhou, W. C. Poh and P. S. Lee, *Sci. Adv.*, 2021, **7**, eabg8433.

70 S. Ding, J. Ying, F. Chen, L. Fu, Y. Lv, S. Zhao and G. Ji, *J. Nanopart. Res.*, 2021, **23**, 1–6.

71 H. S. Lee, Y. Jo, J. H. Joo, K. Woo, Z. Zhong, S. Jung, S. Y. Lee, Y. Choi and S. Jeong, *ACS Appl. Mater. Interfaces*, 2019, **11**, 12622–12631.

72 I. S. Yoon, Y. Oh, S. H. Kim, J. Choi, Y. Hwang, C. H. Park and B.-K. Ju, *Adv. Mater. Technol.*, 2019, **4**, 1900363.

73 I. S. Yoon, S. H. Kim, Y. Oh, B.-K. Ju and J.-M. Hong, *Sci. Rep.*, 2020, **10**, 5036.

74 G. Shin, S. Lee and Y.-L. Park, *IEEE Robot. Autom. Lett.*, 2022, **7**, 4983–4990.

75 B. Kim, A. H. Soepriatna, W. Park, H. Moon, A. Cox, J. Zhao, N. S. Gupta, C. H. Park, K. Kim, Y. Jeon, H. Jang, D. R. Kim, H. Lee, K.-S. Lee, C. J. Goergen and C. H. Lee, *Nat. Commun.*, 2021, **12**, 3710.

76 G. Chen, R. Rastak, Y. Wang, H. Yan, V. Feig, Y. Liu, Y. Jiang, S. Chen, F. Lian, F. Molina-Lopez, L. Jin, K. Cui, J. W. Chung, E. Pop, C. Linder and Z. Bao, *Matter*, 2019, **1**, 205–218.

77 M. Chen, L. Zhang, S. Duan, S. Jing, H. Jiang and C. Li, *Adv. Funct. Mater.*, 2014, **24**, 7548–7556.

78 B.-J. Kim, Y. Cho, M.-S. Jung, H.-A.-S. Shin, M.-W. Moon, H. N. Han, K. T. Nam, Y.-C. Joo and I.-S. Choi, *Small*, 2012, **8**, 3300–3306.

79 H. Hwang, M. Kong, K. Kim, D. Park, S. Lee, S. Park, H.-J. Song and U. Jeong, *Sci. Adv.*, 2021, **7**, eabh0171.

80 T. Lu, J. Wissman, Ruthika and C. Majidi, *ACS Appl. Mater. Interfaces*, 2015, **7**, 26923–26929.

81 Z. Fu, V. Panula, B. Khorramdel and M. Mäntysalo, *Microelectron. Reliab.*, 2021, **119**, 114067.

82 I. Mir and D. Kumar, *Int. J. Adhes. Adhes.*, 2008, **28**, 362–371.

83 R. Aradhana, S. Mohanty and S. K. Nayak, *Int. J. Adhes. Adhes.*, 2020, **99**, 102596.

84 Z. Li, T. Le, Z. Wu, Y. Yao, L. Li, M. Tentzeris, K.-S. Moon and C. P. Wong, *Adv. Funct. Mater.*, 2015, **25**, 464–470.

85 Y. Ko, J. Oh, K. T. Park, S. Kim, W. Huh, B. J. Sung, J. A. Lim, S.-S. Lee and H. Kim, *ACS Appl. Mater. Interfaces*, 2019, **11**, 37043–37050.

86 J. Dou, L. Tang, L. Mou, R. Zhang and X. Jiang, *Compos. Sci. Technol.*, 2020, **197**, 108237.

87 M. H. Behfar, B. Khorramdel, A. Korhonen, E. Jansson, A. Leinonen, M. Tuomikoski and M. Mäntysalo, *Adv. Eng. Mater.*, 2021, **23**, 2100264.

88 J. Luo, Z. Cheng, C. Li, L. Wang, C. Yu, Y. Zhao, M. Chen, Q. Li and Y. Yao, *Compos. Sci. Technol.*, 2016, **129**, 191–197.

89 W. Yuan, X. Wu, W. Gu, J. Lin and Z. Cui, *J. Semicond.*, 2018, **39**, 015002.

90 C. A. Silva, J. Lv, L. Yin, I. Jeerapan, G. Innocenzi, F. Soto, Y.-G. Ha and J. Wang, *Adv. Funct. Mater.*, 2020, **30**, 2002041.

91 X. Chen, L. Yin, J. Lv, A. J. Gross, M. Le, N. G. Gutierrez, Y. Li, I. Jeerapan, F. Giroud, A. Berezovska, R. K. O'Reilly, S. Xu, S. Cosnier and J. Wang, *Adv. Funct. Mater.*, 2019, **29**, 1905785.

92 L. Yin, K. N. Kim, J. Lv, F. Tehrani, M. Lin, Z. Lin, J.-M. Moon, J. Ma, J. Yu, S. Xu and J. Wang, *Nat. Commun.*, 2021, **12**, 1542.

93 J. Lv, L. Yin, X. Chen, I. Jeerapan, C. A. Silva, Y. Li, M. Le, Z. Lin, L. Wang, A. Trifonov, S. Xu, S. Cosnier and J. Wang, *Adv. Funct. Mater.*, 2021, **31**, 2102915.

94 L. Yin, K. N. Kim, J. Lv, F. Tehrani, M. Lin, Z. Lin, J.-M. Moon, J. Ma, J. Yu, S. Xu and J. Wang, *Nat. Commun.*, 2021, **12**, 1542.

95 M. H. Behfar, D. D. Vito, A. Korhonen, D. Nguyen, B. M. Amin, T. Kurkela, M. Tuomikoski and M. Mäntysalo, *IEEE Trans. Compon., Packag., Manuf. Technol.*, 2021, **11**, 1022–1027.



96 J. C. Yang, S. Lee, B. S. Ma, J. Kim, M. Song, S. Y. Kim, D. W. Kim, T.-S. Kim and S. Park, *Sci. Adv.*, 2022, **8**, eabn3863.

97 P. A. Lopes, B. C. Santos, A. T. de Almeida and M. Tavakoli, *Nat. Commun.*, 2021, **12**, 4666.

98 S. Liu, D. S. Shah and R. Kramer-Bottiglio, *Nat. Mater.*, 2021, **20**, 851–858.

99 K. B. Ozutemiz, J. Wissman, O. B. Ozdoganlar and C. Majidi, *Adv. Mater. Interfaces*, 2018, **5**, 1701596.

100 E. Oh, T. Kim, J. Yoon, S. Lee, D. Kim, B. Lee, J. Byun, H. Cho, J. Ha and Y. Hong, *Adv. Funct. Mater.*, 2018, **28**, 1806014.

101 P. Ahlberg, S. H. Jeong, M. Jiao, Z. Wu, U. Jansson, S.-L. Zhang and Z.-B. Zhang, *IEEE Trans. Electron Devices*, 2014, **61**, 2996–3000.

102 M. Péter, D. van den Ende, B. van Remoortere, S. Van Put, T. Podprocky, A. Henckens and J. van den Brand, in *2013 European Microelectronics Packaging Conference (EMPC)*, IEEE, 2013, pp. 1–6.

103 J. Kawahara, P. Andersson Ersman, D. Nilsson, K. Katoh, Y. Nakata, M. Sandberg, M. Nilsson, G. Gustafsson and M. Berggren, *J. Polym. Sci., Part B: Polym. Phys.*, 2013, **51**, 265–271.

104 M. Kujala, T. Kololuoma, J. Keskinen, D. Lupo, M. Mäntysalo and T. M. Kraft, in *2018 International Flexible Electronics Technology Conference (IFETC)*, 2018, pp. 1–6.

105 S. Park, H. Lee, Y.-J. Kim and P. S. Lee, *NPG Asia Mater.*, 2018, **10**, 959–969.

106 S. Ravi-Kumar, B. Lies, X. Zhang, H. Lyu and H. Qin, *Polym. Int.*, 2019, **68**, 1391–1401.

107 Z. Huang, Y. Hao, Y. Li, H. Hu, C. Wang, A. Nomoto, T. Pan, Y. Gu, Y. Chen, T. Zhang, W. Li, Y. Lei, N. Kim, C. Wang, L. Zhang, J. W. Ward, A. Maralani, X. Li, M. F. Durstock, A. Pisano, Y. Lin and S. Xu, *Nat. Electron.*, 2018, **1**, 473–480.

108 P. Ren and J. Dong, *Adv. Mater. Technol.*, 2021, **6**, 2100280.

109 F. Molina-Lopez, T. Z. Gao, U. Kraft, C. Zhu, T. Öhlund, R. Pfattner, V. R. Feig, Y. Kim, S. Wang, Y. Yun and Z. Bao, *Nat. Commun.*, 2019, **10**, 2676.

110 E. Oh, J. Byun, B. Lee, S. Kim, D. Kim, J. Yoon and Y. Hong, *Adv. Electron. Mater.*, 2017, **3**, 1600517.

111 E. Jansson, A. Korhonen, M. Hietala and T. Kololuoma, *J. Adv. Manuf. Technol.*, 2020, **111**, 3017–3027.

112 L. F. Cabeza, in *Advances in Thermal Energy Storage Systems*, Elsevier, 2021, pp. 37–54.

113 C. Pan, Y. Ohm, J. Wang, M. J. Ford, K. Kumar, S. Kumar and C. Majidi, *ACS Appl. Mater. Interfaces*, 2019, **11**, 42561–42570.

114 B. Sun and X. Huang, *npj Flexible Electron.*, 2021, **5**, 1–5.

115 C. Tan, Z. Dong, Y. Li, H. Zhao, X. Huang, Z. Zhou, J.-W. Jiang, Y.-Z. Long, P. Jiang, T.-Y. Zhang and B. Sun, *Nat. Commun.*, 2020, **11**, 3530.

116 S. J. Kang, H. Hong, C. Jeong, J. S. Lee, H. Ryu, J. Yang, J. U. Kim, Y. J. Shin and T. Kim, *Nano Res.*, 2021, **14**, 3253–3259.

117 J. Chen, X. Huang, Y. Zhu and P. Jiang, *Adv. Funct. Mater.*, 2017, **27**, 1604754.

118 S. Bhanushali, P. C. Ghosh, G. P. Simon and W. Cheng, *Adv. Mater. Interfaces*, 2017, **4**, 1700387.

119 D. D. L. Chung, *J. Mater. Eng. Perform.*, 2001, **10**, 56–59.

120 Y. Cui, M. Li and Y. Hu, *J. Mater. Chem. C*, 2020, **8**, 10568–10586.

121 H. Ma and J. C. Suhling, *J. Mater. Sci.*, 2009, **44**, 1141–1158.

122 Y. Yao, X. Zeng, K. Guo, R. Sun and J. Xu, *Composites, Part A*, 2015, **69**, 49–55.

123 C. F. Deng, Y. X. Ma, P. Zhang, X. X. Zhang and D. Z. Wang, *Mater. Lett.*, 2008, **62**, 2301–2303.

124 S. Wang, Y. Cheng, R. Wang, J. Sun and L. Gao, *ACS Appl. Mater. Interfaces*, 2014, **6**, 6481–6486.

125 K. Pashayi, H. R. Fard, F. Lai, S. Iravanti, J. Plawsky and T. Borca-Tasciuc, *Nanoscale*, 2014, **6**, 4292–4296.

126 D. Kuang, L. Xu, L. Liu, W. Hu and Y. Wu, *Appl. Surf. Sci.*, 2013, **273**, 484–490.

127 Y. Cui, Z. Qin, H. Wu, M. Li and Y. Hu, *Nat. Commun.*, 2021, **12**, 1284.

128 B. A. Cola, J. Xu, C. Cheng, X. Xu, T. S. Fisher and H. Hu, *J. Appl. Phys.*, 2007, **101**, 054313.

129 W. Gong, P. Li, Y. Zhang, X. Feng, J. Major, D. DeVoto, P. Paret, C. King, S. Narumanchi and S. Shen, *Nano Lett.*, 2018, **18**, 3586–3592.

130 A. A. Balandin, *Nat. Mater.*, 2011, **10**, 569–581.

131 D. Kumlutaş, İ. H. Tavman and M. Turhan Çoban, *Compos. Sci. Technol.*, 2003, **63**, 113–117.

132 H. S. Tekce, D. Kumlutaş and I. H. Tavman, *J. Reinf. Plast. Compos.*, 2007, **26**, 113–121.

133 A. Boudenne, L. Ibos, M. Fois, J. C. Majesté and E. Géhin, *Composites, Part A*, 2005, **36**, 1545–1554.

134 Ye. P. Mamunya, V. V. Davydenko, P. Pissis and E. V. Lebedev, *Eur. Polym. J.*, 2002, **38**, 1887–1897.

135 N. Bagotia, V. Choudhary and D. K. Sharma, *Polym. Adv. Technol.*, 2018, **29**, 1547–1567.

136 E.-C. Cho, C.-W. Chang-Jian, Y.-S. Hsiao, K.-C. Lee and J.-H. Huang, *Composites, Part A*, 2016, **90**, 678–686.

137 S. Shen, A. Henry, J. Tong, R. Zheng and G. Chen, *Nat. Nanotechnol.*, 2010, **5**, 251–255.

138 H. Bark, M. W. M. Tan, G. Thangavel and P. S. Lee, *Adv. Energy Mater.*, 2021, **11**, 2101387.

139 A. J. McNamara, Y. Joshi and Z. M. Zhang, *Int. J. Therm. Sci.*, 2012, **62**, 2–11.

140 H. S. Kim, J. Jang, H. Lee, S. Y. Kim, S. H. Kim, J. Kim, Y. C. Jung and B. J. Yang, *Adv. Eng. Mater.*, 2018, **20**, 1800204.

141 H. Jiang, Z. Wang, H. Geng, X. Song, H. Zeng and C. Zhi, *ACS Appl. Mater. Interfaces*, 2017, **9**, 10078–10084.

142 Z. Wang, Y. Fu, W. Meng and C. Zhi, *Nanoscale Res. Lett.*, 2014, **9**, 643.

143 W. Chen, Z. Wang, C. Zhi and W. Zhang, *Compos. Sci. Technol.*, 2016, **130**, 63–69.

144 C. P. Wong and R. S. Bollampally, *J. Appl. Polym. Sci.*, 1999, **74**, 3396–3403.



145 F. Zhang, Y. Feng and W. Feng, *Mater. Sci. Eng., R*, 2020, **142**, 100580.

146 H. Khakbaz, K. Ruberu, L. Kang, S. Talebian, S. Sayyar, B. Filippi, M. Khatamifar, S. Beirne and P. C. Innis, *J. Mater. Sci.*, 2021, **56**, 6385–6400.

147 L. Chen, Y.-Y. Sun, J. Lin, X.-Z. Du, G.-S. Wei, S.-J. He and S. Nazarenko, *Int. J. Heat Mass Transfer*, 2015, **81**, 457–464.

148 H. Yuan, Y. Wang, T. Li, Y. Wang, P. Ma, H. Zhang, W. Yang, M. Chen and W. Dong, *Nanoscale*, 2019, **11**, 11360–11368.

149 T. Gao, Z. Yang, C. Chen, Y. Li, K. Fu, J. Dai, E. M. Hitz, H. Xie, B. Liu, J. Song, B. Yang and L. Hu, *ACS Nano*, 2017, **11**, 11513–11520.

150 X. Zhou, K. Parida, O. Halevi, Y. Liu, J. Xiong, S. Magdassi and P. S. Lee, *Nano Energy*, 2020, **72**, 104676.

151 Z. Wang, J. Fan, D. He, L. Ren, Z. Hao, R. Sun and X. Zeng, *J. Mater. Chem. A*, 2022, **10**, 21923–21932.

152 H. Aglan, M. Calhoun and L. Allie, *J. Appl. Polym. Sci.*, 2008, **108**, 558–564.

153 P. Costa, S. Ribeiro, G. Botelho, A. V. Machado and S. Lanceros Mendez, *Polym. Test.*, 2015, **42**, 225–233.

154 D. Qi, K. Zhang, G. Tian, B. Jiang and Y. Huang, *Adv. Mater.*, 2021, **33**, 2003155.

155 I. You, M. Kong and U. Jeong, *Acc. Chem. Res.*, 2019, **52**, 63–72.

156 J. Wang, G. Cai, S. Li, D. Gao, J. Xiong and P. S. Lee, *Adv. Mater.*, 2018, **30**, 1706157.

157 H. Bark and P. See Lee, *Chem. Sci.*, 2021, **12**, 2760–2777.

158 Q. Jiang, S. Zhang, J. Jiang, W. Fei and Z. Wu, *Adv. Mater. Technol.*, 2021, **6**, 2000966.

159 K. Kim, H. J. Kim, H. Zhang, W. Park, D. Meyer, M. K. Kim, B. Kim, H. Park, B. Xu, P. Kollbaum, B. W. Boudouris and C. H. Lee, *Nat. Commun.*, 2021, **12**, 1544.

160 S. Choi, S. I. Han, D. Jung, H. J. Hwang, C. Lim, S. Bae, O. K. Park, C. M. Tschabrunn, M. Lee, S. Y. Bae, J. W. Yu, J. H. Ryu, S.-W. Lee, K. Park, P. M. Kang, W. B. Lee, R. Nezafat, T. Hyeon and D.-H. Kim, *Nat. Nanotechnol.*, 2018, **13**, 1048–1056.

161 Y. Wang, J. Kong, R. Xue, J. Wang, M. Gong, X. Lin, L. Zhang and D. Wang, *Nano Res.*, 2022, DOI: **10.1007/s12274-022-4757-9**.

162 H. Lee, S. Hong, J. Lee, Y. D. Suh, J. Kwon, H. Moon, H. Kim, J. Yeo and S. H. Ko, *ACS Appl. Mater. Interfaces*, 2016, **8**, 15449–15458.

163 S. Park, A. W. Ming Tan, J. Wang and P. See Lee, *Nanoscale Horiz.*, 2017, **2**, 199–204.

164 J. H. Song, Y.-T. Kim, J.-B. Seol, C.-G. Park, J.-M. Myoung and U. Jeong, *Adv. Mater. Interfaces*, 2018, **5**, 1800250.

165 S. Huang, Y. Liu, M. Jafari, M. Siaj, H. Wang, S. Xiao and D. Ma, *Adv. Funct. Mater.*, 2021, **31**, 2010022.

166 T. Araki, T. Sugahara, M. Nogi and K. Saganuma, *Jpn. J. Appl. Phys.*, 2012, **51**, 11PD01.

167 G. Cai, S. Park, X. Cheng, A. L.-S. Eh and P. S. Lee, *Sci. Technol. Adv. Mater.*, 2018, **19**, 759–770.

168 S. Oprea and V. Oprea, *Eur. Polym. J.*, 2002, **38**, 1205–1210.

169 A. Boubakri, N. Guermazi, K. Elleuch and H. F. Ayedi, *Mater. Sci. Eng., A*, 2010, **527**, 1649–1654.

170 A. Boubakri, N. Haddar, K. Elleuch and Y. Bienvenu, *Mater. Des.*, 2010, **31**, 4194–4201.

171 G. Theiler, V. Wachtendorf, A. Elert and S. Weidner, *Polym. Test.*, 2018, **70**, 467–473.

172 B. Venkatesulu and M. J. Thomas, *IEEE Trans. Dielectr. Electr. Insul.*, 2011, **18**, 418–424.

173 P. N. Eleni, M. K. Krokida, G. L. Polyzois, C. A. Charitidis, E. P. Koumoulos, V. P. Tsikourkitoudi and I. Ziomas, *Polym. Degrad. Stab.*, 2011, **96**, 470–476.

174 P. N. Eleni, M. K. Krokida and G. L. Polyzois, *Biomed. Mater.*, 2009, **4**, 035001.

175 C. C. White, K. T. Tan, D. L. Hunston, T. Nguyen, D. J. Benatti, D. Stanley and J. W. Chin, *Polym. Degrad. Stab.*, 2011, **96**, 1104–1110.

176 X. Li, J. Gao, Q. Zhao, J. Bao, X. Hu and G. Wang, *J. Appl. Polym. Sci.*, 2008, **110**, 3820–3825.

177 M. Liu and A. R. Horrocks, *Polym. Degrad. Stab.*, 2002, **75**, 485–499.

178 M. Sang, K. Kim, J. Shin and K. J. Yu, *Adv. Sci.*, 2022, **9**, 2202980.

179 P. Le Floch, S. Meixuanzi, J. Tang, J. Liu and Z. Suo, *ACS Appl. Mater. Interfaces*, 2018, **10**, 27333–27343.

180 L. Yin, J. Scharf, J. Ma, J.-M. Doux, C. Redquest, V. L. Le, Y. Yin, J. Ortega, X. Wei, J. Wang and Y. S. Meng, *Joule*, 2021, **5**, 228–248.

181 P. C. Hiemenz and T. P. Lodge, *Polymer chemistry*, CRC press, 2007.

182 A. Vohra, H. L. Filiatrault, S. D. Amyotte, R. S. Carmichael, N. D. Suhan, C. Siegers, L. Ferrari, G. J. E. Davidson and T. B. Carmichael, *Adv. Funct. Mater.*, 2016, **26**, 5222–5229.

183 A. Vohra, R. S. Carmichael and T. B. Carmichael, *Langmuir*, 2016, **32**, 10206–10212.

184 Y. Shao, S. Yan, J. Li, Z. Silva-Pedraza, T. Zhou, M. Hsieh, B. Liu, T. Li, L. Gu, Y. Zhao, Y. Dong, B. Yin and X. Wang, *ACS Appl. Mater. Interfaces*, 2022, **14**, 18935–18943.

185 A. Vohra, K. Schlingman, R. S. Carmichael and T. B. Carmichael, *Chem*, 2018, **4**, 1673–1684.

186 H. Yang, C. Li and J. Tang, *Extreme Mech. Lett.*, 2022, **54**, 101761.

187 L. Gillan, J. Hiltunen, M. H. Behfar and K. Rönkä, *Jpn. J. Appl. Phys.*, 2022, **61**, SE0804.

